Pergamon

Planet. Space Sci., Vol. 44, No. 9, pp. 945–955, 1996

0032–0633/96 $15.00+0.00

PII: S0032-0633(96)00001-3

The emissivity of volatile ices on Triton and Pluto

John A. Stansberry,[1] D. J. Pisano[2] and Roger V. Yelle[3]

[1] Lowell Observatory, Flagstaff, AZ 86001, U.S.A.
[2] Yale University, Department of Astronomy, New Haven, CT 06520, U.S.A.
[3] Boston University, Astronomy Department, Boston, MA 02215, U.S.A.

Received 5 May 1995; revised 18 December 1995; accepted 18 December 1995

Abstract. The Hapke theory is used to calculate the emissivity of a semi-infinite layer of granular N_2 ice with CH_4 and CO as contaminants. It is assumed that the layer is composed of grains which can be characterized as having a single size, and that temperature gradients in the emitting layers of the surface are negligible. The emission spectrum for β-N_2, stable above 35.6 K, results from a very broad peak in the absorption spectrum centered at 154 μm, while two absorption peaks, at 143 and 204 μm, produce the emission spectrum of the lower temperature α-N_2 phase. For a grain size of 1 cm the Planck-mean bolometric emissivity calculated for the pure β-N_2 ice is 0.85. If the effective N_2 grain size is 1 mm the emissivity is 0.40. Both are low enough to significantly affect surface energy balance calculations. The very narrow absorption features of α-N_2 result in even smaller bolometric emissivities of only 0.11 and 0.30 for 1 mm and 1 cm grain sizes at 34 K. The effect of CH_4 and CO, in solid solution with N_2 or as separate, intimately mixed grains, on the emissivity is also estimated. It is found that the presence of either or both of these two molecules in solid solution with the N_2 ice on Triton and Pluto only slightly increases the β-N_2 emissivity. The emissivity of intimate mixtures of grains of CH_4 and CO with N_2 is much less certain, and probably much less applicable to Triton and Pluto. CH_4 and CO in solid solution with α-N_2 increase the emissivity by about 50%. For an α-N_2 grain size of 1 cm, the addition of 2% each CH_4 and CO in solid solution with the N_2 increases the emissivity from 0.30 to 0.48 at 34 K. For a 1 mm grain size the emissivity of such a solid solution changes to 0.16 from 0.11. However, the emissivity of α-N_2 even with CH_4 and/or CO in solution is still considerably lower than for β-N_2. Seasonal variations on Triton and Pluto could be strongly influenced by this emissivity contrast between the α and β phases. In the extreme case of pure N_2 ice, Pluto's atmosphere could be prevented from freezing out, even at aphelion.

Introduction

The emissivity of N_2 ice has been an issue since shortly after the 1989 Voyager 2 encounter with Neptune and Triton. The kinetic temperature of Triton's N_2 ice is tightly constrained by measurements of the atmospheric pressure. This follows from the fact that the N_2 atmosphere is in vapor pressure equilibrium with the ice on the surface, and that the atmosphere is also thick enough to have an essentially uniform pressure globally (Trafton and Stern, 1983; Ingersoll, 1990; Stansberry, 1994; Yelle *et al.*, 1995). Together with the strong temperature dependence of the N_2 vapor pressure curve (Brown and Ziegler, 1980), the Voyager Radio Science Subsystem (RSS) surface pressure determination for Triton, 14 ± 1 μb (Gurrola, 1995; cf. Tyler *et al.*, 1989; Broadfoot *et al.*, 1989; Yelle *et al.*, 1991) translates into a temperature for the N_2 ice of 37.5 ± 0.12 K. This temperature determination is in excellent agreement with the recent results of Tryka *et al.* (1993) and Grundy *et al.* (1993), who measured the temperature dependent shape of the 2.16 μm N_2 ice absorption band and compared their lab data to the feature in telescopic spectra of Triton. Tryka *et al.* concluded that the temperature of Triton's N_2 ice is 38 ± 1 K, while Grundy *et al.* obtained their best fit for a temperature in the range 35.6–38 K.

These studies determine the kinetic temperature of N_2 ice on Triton, however, both the brightness temperature of Triton and the temperature implied by Triton's albedo are significantly colder than 37.5 K. Triton's thermal emission was directly detected using the Infrared Interferometer Spectrometer (IRIS) on Voyager (Conrath *et*

Correspondence to: J. A. Stansberry

al., 1989). An average of 16 dayside spectra provided a unit emissivity brightness temperature of 38^{+3}_{-4} K, consistent with the determination based on atmospheric pressure, but with a much larger uncertainty. Another uncertainty associated with the IRIS spectra is whether they pertained to the temperature of the N_2 ice or to other surface materials. A more thorough analysis of the IRIS data (Stansberry *et al.*, 1996b) using over 90 spectra from both day and night side found an average unit emissivity brightness temperature $\simeq 34$ K. Taking the kinetic temperature to be 37.5 K, consistent with the RSS determined atmospheric pressure, Stansberry *et al.* find a best fit emissivity of 0.42 ± 0.07.

A second line of evidence for a low emissivity comes from energy balance studies based on the Voyager Imaging Science Subsystem (ISS) data (Hillier *et al.*, 1990, 1991; Stansberry *et al.*, 1990, 1992). These studies conclude that Triton reflects too much sunlight to have a temperature as high as 37.5 K if the emissivity is near unity, and have proposed emissivities for the N_2 ice in the range 0.30–0.77. These values are well below unity, in qualitative agreement with the analysis of the IRIS data. A second effect to consider in Triton's surface energy balance is internal heat flow. Brown and Kirk (1991) show that the contribution of internal heat to the globally averaged energy budget is between 5 and 20% of the insolation. This would increase surface temperatures by 0.5–1.5 K over the value calculated by considering only insolation and reradiation, thus reducing but not eliminating the need for N_2 ice on Triton to have a low emissivity. On the other hand, including internal heat flow would require even lower emissivities for the N_2 ice in order to explain the low brightness temperatures measured by IRIS.

The emissivities just discussed are significantly lower than the typical values (in the range 0.9–1) assumed for warmer planets, and have generated some skepticism. One objection is based on measurements of Triton's albedo taken with the Voyager Photopolarimeter Spectrometer (PPS) (Nelson *et al.*, 1990a,b). The PPS albedos are about 20% lower than those derived from the ISS data, and yield surface temperatures of approximately 38 K for an emissivity of one. Secondly, Nelson *et al.* (1990a,b) and Eluszkiewicz (1991) have argued that if the surface of the N_2 ice on Triton is rough at scales comparable to or greater than the wavelength of the blackbody peak, $\sim 100\,\mu$m, then the surface will behave as if it is covered with cavity radiators and the emissivity will be near unity. Stansberry (1994) and Stansberry *et al.* (1996b) have argued against this cavity radiator paradigm, and we will briefly discuss some of those arguments below.

Nearly all of the information we have concerning the emissivity of N_2 ice comes from studies of Triton. Pluto's surface is also dominated by N_2 ice (Owen *et al.*, 1993), but the constraints on its temperature are far less stringent than on Triton. The atmospheric pressure at a reference radius of 1250 km from Pluto's center, $1.2 \pm 0.25\,\mu$b, was determined from the 1988 observation of Pluto occulting a star (Hubbard *et al.*, 1989, 1990; Elliot *et al.*, 1989; Elliot and Young, 1992; Millis *et al.*, 1993; Young, 1994), but Pluto's surface lies well below 1250 km. The deepest penetration of the occultation into the atmosphere was at a radius of approximately 1200 km (Young, 1994; Stansberry *et al.*, 1994), and the surface was not detected. Thus, Pluto's surface pressure, unlike Triton's, is very uncertain, with the occultation only providing a lower bound on the surface pressure of $P_0 > 3\,\mu$b. The actual surface pressure depends on Pluto's true radius and the details of the atmospheric temperature profile below 1250 km which are not precisely known.

Stansberry *et al.* (1994) calculated surface pressures in the range 3–24 μb, taking 1198 km as the radius of deepest penetration in the occultation, and 1158 km (an average of the mutual event radius determinations of Buie *et al.* (1992) and Young and Binzel (1994)) as the lower limit on the radius. One suite of models explored by Young (1994), using the formal error on the Young and Binzel mutual event radius to determine a lower bound on Pluto's radius (1133 km), determines a range of surface pressures of 3.9–160 μb. Due to the extreme dependence on temperature of the N_2 vapor pressure curve (Brown and Ziegler, 1980), these pressure uncertainties translate into N_2 ice temperature uncertainties of only 35.1–38.4 and 35.5–42.0 K, respectively.

Tryka *et al.* (1994) have analyzed spectra of Pluto as well as of Triton and, applying the same method mentioned earlier, conclude that Pluto's N_2 ice has a temperature of 40 ± 2 K with corresponding surface pressures in the range 20–160 μb. These pressures agree nicely with the models of Young (1994) and overlap the upper end of the range proposed by Stansberry *et al.* (1994). Tryka *et al.* have also shown that Pluto's thermal emission, measured by various authors over the wavelength range 25–1300 μm, can be modeled assuming Pluto has isothermal N_2 ice polar caps with an emissivity of 0.6 and a temperature of 40 K. Pluto's albedo distribution has been modeled using observations of the mutual eclipses between it and its moon, Charon (Buie *et al.*, 1992; Young, 1993; Reinsch *et al.*, 1994; Drish *et al.*, 1995). Stansberry *et al.* (1994) used the Buie *et al.* and the Young albedo maps to calculate Pluto's surface energy balance. Although emissivity values for various surface pressures were not explicitly reported in that paper, they were an integral part of those calculations. For N_2 ice temperatures in the range 38–40 K emissivities were found to be $\simeq 0.6$, similar to the values calculated for Triton.

Models of the near-IR spectra of Triton and Pluto show that both surfaces are dominated by N_2 ice. The size of the N_2 grains is $\simeq 1$ cm (Grundy and Fink, 1991; Cruikshank *et al.*, 1993; Owen *et al.*, 1993; Grundy *et al.*, 1993; Grundy, 1995). Tryka *et al.* (1993, 1994) find somewhat smaller grain sizes on Triton and Pluto, achieving their best fit to the spectra with 0.3–0.4 cm grains on Triton, and $\simeq 0.15$ cm grains on Pluto. It should be noted that all of these models derive an "effective" grain size, which is really just the average distance between scattering centers in the ice. It is not entirely clear what structures within the ice are really scattering the radiation (it could be bubbles as easily as grain boundaries), and it is improbable that the surface is composed of grains of a single size. However, given these caveats, models of the near-IR spectrum give us the best estimates we have of what the effective grain size is in the far-IR.

The Owen *et al.* (1993) and Cruikshank *et al.* (1993) spectroscopic studies also found that CH_4 is present as a

minor species in the volatile layers of both bodies ($\simeq 0.5\%$ by mass on Triton, $\simeq 1.5\%$ on Pluto). CO has also been observed in the spectrum of both bodies, and they estimate the abundance is a few tenths of a percent on either. Other ingredients certain to be present in or on Triton's and Pluto's N_2 ice are hydrocarbons produced by photolysis of CH_4 in the atmosphere or within the surface. These probably produce the reddish tint of some areas on Triton (McEwen, 1990; Thompson and Sagan, 1990), and may be the dark material observed in some areas on both bodies (Smith *et al.*, 1989; Buie *et al.*, 1992; Young and Binzel, 1994; Reinsch *et al.*, 1994; Drish *et al.*, 1995).

We approach the calculation of the emissivity of N_2 ice on Triton and Pluto in two stages. We first present models for a surface composed of pure N_2 ice grains. We then present a series of models to assess the importance of CH_4 and CO as contaminants in the ice. We also include as a possibility other materials, modeled as a grey absorber either in solid solution or as dispersed particles within the surface, in an attempt to include the effect of photochemical products on the emissivity. We then discuss the model results in the context of the various observational constraints introduced above, and lay out the implications for energy balance and seasonal variability on Triton and Pluto.

Emissivity calculation

We use Hapke theory to calculate the emissivity of a surface composed of N_2 ice. The theory is typically used for calculating the reflectance of particulate surfaces (Hapke, 1981, 1986), but has been extended to the case of thermal emission in more recent work (Hapke, 1993). The expression for the directional emissivity, assuming the surface is composed of isotropic scatterers, is simply

$$\varepsilon_d = \gamma H(\mu, w) \tag{1}$$

where $\gamma = \sqrt{1-w}$, and the hemispherical emissivity is

$$\varepsilon_h = 2\gamma \int_0^1 H(\mu, w)\mu \, d\mu$$

$$\simeq \frac{2\gamma}{1+\gamma}\left(1+\frac{r_0}{6}\right). \tag{2}$$

These expressions are equations (13.19), (13.23) and (13.24) of Hapke (1993). H is the Chandrasekhar H function for isotropic scatterers describing multiple scattering, μ the cosine of the emission angle, w the wavelength dependent single scattering albedo of the particles which make up the surface, and the diffusive reflectance, $r_0 = (1-\gamma)/(1+\gamma)$ (Hapke, 1993, equation (8.25)). We numerically evaluated the integral $\int_0^1 H(\mu)\mu \, d\mu$ using the tabulation of Hiroi (1994) for H and found that the approximation in equation (2) is accurate to within 1%. These expressions allow us to calculate the emissivity given the single scattering albedo of the N_2 ice grains comprising the surface.

We calculate the single scattering albedos of spherical particles of N_2 ice using Mie theory (Van de Hulst, 1957) for small particles ($X = 2\pi\alpha/\lambda \leq 100$, where α is the particle size and λ the wavelength). Typically Mie theory is used up to $X = 400$, and geometric optics used beyond that. However, one of the basic results of geometric optics for large isolated particles is that the extinction efficiency for a sphere, $Q_{ext} = 2$. However, setting $Q_{ext} = 2$ leads to an erroneous upper limit in the emissivity calculated for a surface composed of large particles. As Hapke (1993, chapter 7) points out, in a medium composed of large, closely packed particles, the effects of diffraction become negligible and the extinction efficiency of the particles should be $Q_{ext} = 1$. We require Q_{ext} to change smoothly from 2 at $X = 10$ to 1 for $X \gtrsim 400$ according to the bridging formula

$$Q_{ext} = 1.5 + \frac{1}{2}\cos\left(\frac{\pi}{400}(X-10)\right); \quad 10 < X < 410. \tag{3}$$

We experimented with forms for Q_{ext} which changed over other ranges in X which were wider, narrower and had different centers, but found that the changes in the Planck mean emissivities (see below) we calculated were only a few percent. We selected this form because it provided results which were representative of the cases we tried, while containing the essentials of the physics for closely packed particles. The single scattering efficiencies also do not strictly apply for surfaces composed of very small ($X < 1$) particles (Hapke, personal communication). We ran models which we set $Q_{ext}(X < 1) = Q_{ext}(X = 1)$ and found very little change in our calculated Planck-mean emissivities (see below), although the spectral emissivity of such surfaces for $\lambda \gtrsim 200\,\mu m$ was diminished significantly. We calculate the single scattering albedo of the particles from $w = Q_{sca}/Q_{ext}$, and $Q_{sca} = Q_{ext} - Q_{abs}$, where Q_{ext} is calculated either from Mie theory or equation (3), and the absorption efficiency, Q_{abs}, is calculated from Mie theory for $X < 100$ or geometric optics for $X > 100$.

Absorption in N_2 *ice*

Our calculation of the far-IR single scattering albedo of N_2 grains starts with the absorption spectrum of N_2 ice, shown in Fig. 1. The absorption coefficients for β-N_2 (line with solid triangles: Buontempo *et al.*, 1979), liquid N_2 (line with open circles: Jones, 1970), and α-N_2 (two sharp peaks: St. Louis and Schnepp, 1969) are shown, as well as a 38 K Planck function. We have used an analytical approximation to the spectrum (heavy solid line) in our calculations of the emissivity of β-N_2:

$$\alpha_\beta = 8.3 \times 10^{-5}\kappa^3 e^{-0.048\kappa} \tag{4a}$$

where κ is the wave number (cm^{-1}). The fit to the β-N_2 data of Bountempo *et al.* is quite good on the short wavelength side of the peak, probably as accurate as our digitization of their figure. On the long wavelength side of the peak our expression overestimates the absorption coefficients for β-N_2 somewhat, so the emissivities we calculate longward of about 250 μm will be slightly too large. This has a very minor effect on the Planck-mean emis-

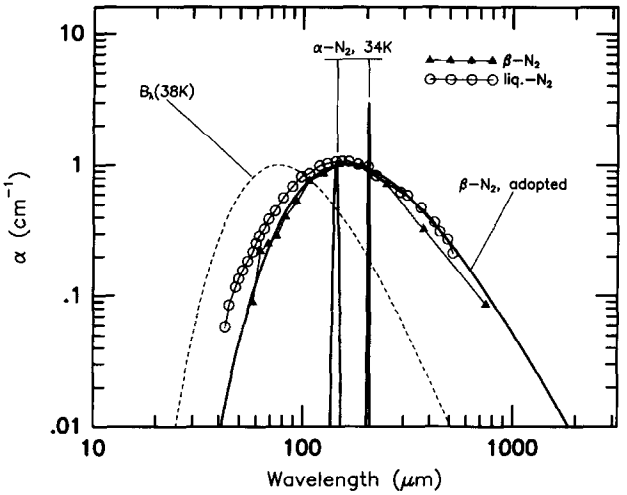

Fig. 1. The absorbtion coefficients of α-, β- and liquid N_2 as a function of wavelength in the far-IR. The heavy solid lines show approximations of the data used in these calculations. The Planck function at 38 K, normalized to 1 at the peak, is shown for comparison

sivities we calculate later because the Planck function is down by over an order of magnitude and dropping as approximately λ^{-4} beyond 250 μm. We chose to use an analytic form for the absorption coefficients of β-N_2 (and other molecules) rather than interpolate the data because the data cover too narrow a wavelength region. By using the analytic forms we obtain an extrapolation outside the region of the data which is consistent with the trends of the data. The more complete wavelength coverage offered by the analytic forms allows us to compute Planck-mean emissivities, which are required for comparison with the energy balance results presented in the Introduction. The details of the extrapolated spectrum do not greatly influence the mean emissivities, but our spectral emissivities should not be relied on too heavily outside the range of the data in Fig. 1.

The spectrum of α-N_2 in Fig. 1 is distinctly different than the β-N_2 spectrum. It is also strongly temperature dependent, while the β-N_2 spectrum is only weakly dependent on temperature (Buontempo *et al.*, 1979). The spectrum shown is for α-N_2 at 34 K, 1.6 K below the phase transition temperature, $T_c = 35.6$ K. St. Louis and Schnepp (1969) reported that the two narrow absorptions seen here grow stronger at lower temperatures, and die out entirely at T_c. More recent measurements (R. Tipping, personal communication) indicate that the spectrum may transition between that of α and β over a temperature range of perhaps as much as 1/2K around T_c. We have modeled the α-N_2 absorption data of St. Louis and Schnepp using the following expressions:

$$\alpha_\alpha = [15.5e^{-[(\kappa-49)/0.25]^2}/2 + 3.9e^{-[(\kappa-70)/1.3]^2}/2]S(T) \quad (4b)$$

$$S(T) = 1 - \frac{(T-15)}{21}. \quad (4c)$$

The two lines are centered at 49 cm^{-1} (204 μm) and 70 cm^{-1} (143 μm), and are 0.25 and 1.3 cm^{-1} in half-width. $S(T)$ specifies the temperature dependent strengths of the two lines.

We assume that the effective grain size in the far-IR is the same as that determined from analyses of the near-IR spectrum discussed earlier. This may not be true if the scattering irregularities which give rise to the near-IR spectra of Triton and Pluto are less effective or more effective at scattering far-IR radiation. We allow for this possibility by calculating the single scattering albedo for particle sizes from 50 μm to 50 cm, but focus our discussion of the results on grain sizes of 0.1–1 cm. For a given particle size the single scattering albedo is calculated for wave numbers from 1 to 500 cm^{-1} (wavelengths $20 < \lambda < 10^4$ μm). These values are then used in equation (2) to calculate the spectral emissivity of a surface composed of particles of that size.

Figure 2a shows the spectral hemispherical emissivity

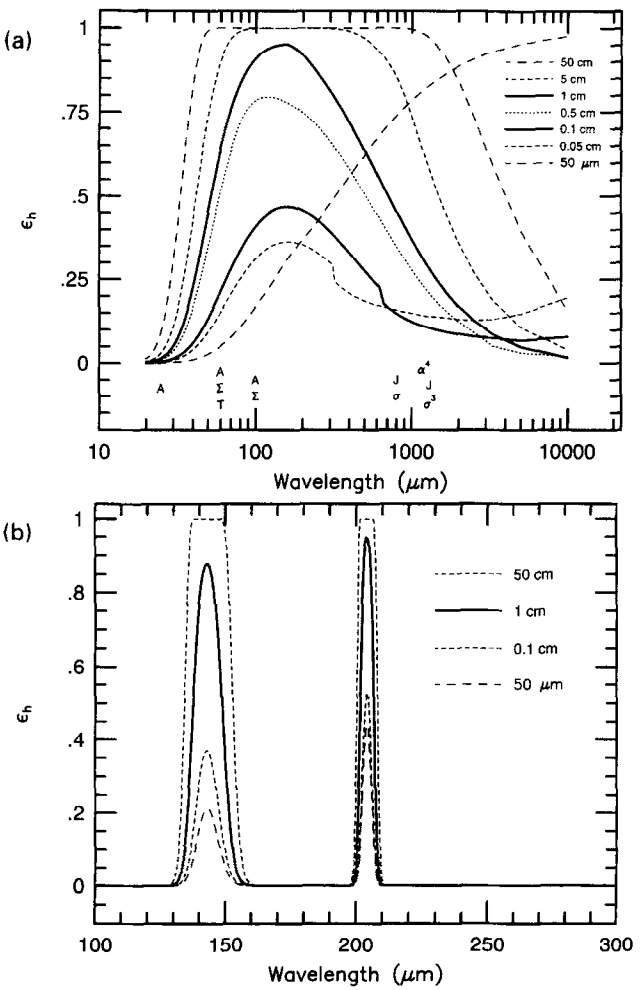

Fig. 2. (a) The hemispherical emissivity of a surface composed of β-N_2 grains as a function of wavelength. The various curves are the calculated emissivity for various particle sizes. Below 120 μm the emissivities increase monotonically with particle size. The letters across the bottom of the figure correspond to far-IR brightness measurements of Pluto by: A, Aumann and Walker (1987); Σ, Sykes *et al.* (1987); T, Tedesco *et al.* (1987); J, Jewitt (1994); σ, Stern *et al.* (1993); α, Altenhoff *et al.* (1988). Superscripts on the letters correspond to the number of reported measurements. (b) The hemispherical emissivity of a surface composed of α-N_2 grains as a function of wavelength for grain sizes of 100 μm, 0.1, 1, and 50 cm

of a β-N_2 surface for the various particle sizes we used in our calculation. The emissivity at a given wavelength increases monotonically with particle size for most of the wavelength range shown. As indicated earlier, the values of ε_h for the 50 μm particles are too large beyond about $\lambda = 200\,\mu$m. The emissivity for the largest particle sizes reaches unity in the region of the absorption peak because the absorption efficiency for the particles, Q_{abs}, approaches one. Kirchhoff's law tells us that the "emission efficiency" for these particles also approaches one. The curves for particle sizes of 0.1 and 1 cm peak at $\varepsilon_h = 0.47$ and 0.95, respectively, and exhibit a strong downward slope shortward of $\sim 100\,\mu$m. The exact location of the peak in emissivity depends somewhat on our choice of bridging formula (equation (3)), but always lies in the 100–200 μm range. The wavelengths at which far-IR measurements of Pluto's surface have been made are marked by the letters at the bottom of Fig. 2a. Triton's thermal radiation was detected at wavelengths shortward of 50 μm by the Voyager 2 IRIS (Conrath *et al.*, 1989; Stansberry *et al.*, 1996b). Implications of these calculations for the observations will be discussed below.

Figure 2b is the spectral emissivity for an α-N_2 surface. Here only four particle sizes are shown: 100 μm, 0.1, 1, and 50 cm. Note that the wavelength scale is linear here, and covers a very restricted region compared with Fig. 2a. The emissivity increases monotonically with particle size in both emission lines for all of the particle sizes we considered. The peak emissivity for 0.1 and 1 cm grain sizes is 0.4 and 0.87 respectively in the 143 μm line, and 0.57 and 0.90 in the 204 μm line. Both lines reach unit emissivity for 5 and 50 cm particle sizes.

Figure 3 shows the bolometric emissivity, ε_b, as a function of temperature for the various particle sizes we considered. The bolometric emissivity is the Planck mean of the hemispherical emissivity and is calulated from

$$\varepsilon_b = \frac{1}{\sigma T^4} \int_0^\infty B(T)\varepsilon_h(\lambda)\,d\lambda \qquad (5)$$

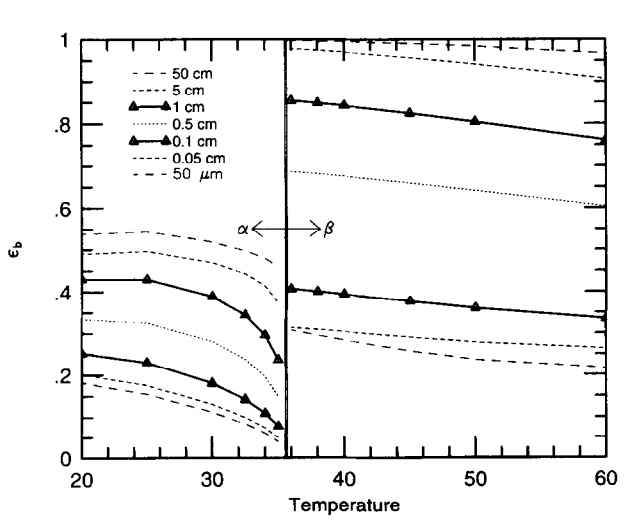

Fig. 3. The Planck-mean hemispherical emissivity as a function of temperature for surfaces having various particle sizes. The figure is split by a vertical double line at 35.6 K, which is the phase transition temperature between α-N_2 and β-N_2. Symbols on the 1 cm curve show the spacing of the calculations

where σ is the Stefan–Boltzmann constant, and B the Planck function. The bolometric emissivity governs the energy balance of the surface given its temperature. Alternatively, the temperature of the surface can be found from its albedo and the insolation using ε_b. In Fig. 3 the double vertical line separates the β-N_2 stability region ($T > 35.6$ K) from the α-N_2 region. For both phases ε_b increases monotonically from the smallest particle size to the largest. For β-N_2, ε_b decreases slowly with increasing temperature due to the change in the Planck function with temperature. For α-N_2 the temperature dependent strength of the absorption lines produces emissivities which decrease as the phase transition temperature, $T_c = 35.6$ K, is approached. We have not calculated the emissivity between 35 and 36 K because we are not certain what the spectrum looks like in that temperature range. There is some evidence that it may be intermediate between the α and β spectrum (R. Tipping, personal communication), or that both α and β exist over some finite temperature range (Prokhvatilav and Yantsavich, 1983). Either way we can safely conclude that the emissivity changes drastically between about 35 and 36 K: the precise details await more data on the spectrum.

For a β-N_2 surface with a 0.1–1 cm effective grain size (heavy lines with triangles) $0.40 \leq \varepsilon_b \leq 0.85$. These values are in excellent agreement with the range of emissivities derived in other studies discussed earlier. In order to reach an emissivity greater than 0.9 with β-N_2, effective grain sizes in the far-IR need only be slightly in excess of 1 cm, but to get $\varepsilon_b \simeq 1$, 5–50 cm grain sizes are required. Although these values do not include the effects of any contaminants in the N_2 ice, it will be shown later that such contaminants do not change these results significantly. If the N_2 ice on Triton or Pluto transitions to the α phase, ε_b will probably be much lower. For 0.1–1 cm grain sizes and $T = 34$ K, ε_b will be in the range 0.11–0.30. At this point there is no real constraint on the size of α grains, but if they form *in situ* from β-N_2 the volume change associated with the phase transition (Scott, 1976) will likely lead to shattering, producing smaller grains and therefore even lower emissivities. Emissivities this low will have a tremendously important effect on the thermal balance of Triton and Pluto when their surfaces are at temperatures below or at the α–β phase transition temperature.

CH_4 and CO

In order to assess the impact of CO, CH_4 and photochemical products on the emissivities just computed we require their optical constants in the far-IR. We have used the absorption spectrum of liquid CH_4 to approximate the solid spectrum because we did not locate adequate data for the ice at wavelengths beyond 25 μm. At temperatures greater than 20.4 K CH_4 exists in a disordered phase (β phase), which is crystallographically similar to β-N_2 (Baran and Medina, 1986). The spectrum of liquid N_2 is very similar to the β-N_2 spectrum in the far-IR (Fig. 1), so the crystallographic similarity between N_2 and CH_4 suggests that the use of the liquid spectrum is a good first approximation. This supposition is supported by the

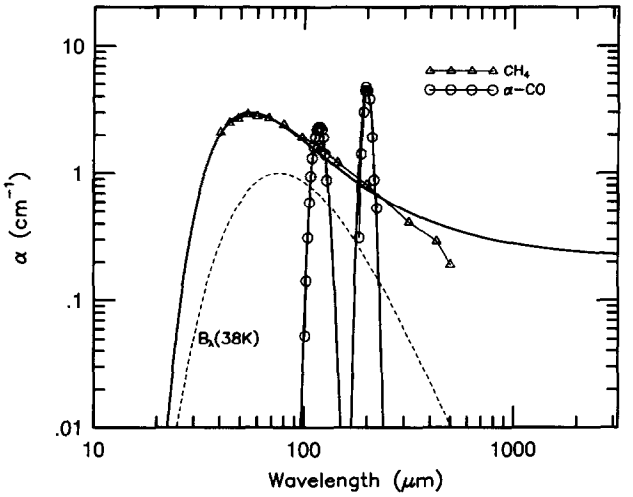

Fig. 4. The measured absorption coefficients of β-CH_4 and α-CO vs. wavelength are plotted as points. The heavy solid lines show our analytic approximations to the data. The dashed line gives the 38 K Planck function normalized to one at the peak

transmission spectra of Savoie and Fournier (1970), which indicate that β-CH_4 is at most 20% more absorbing than the liquid in the 50–200 μm region. CO exists in the ordered α phase at temperatures below 61.6 K. α-CO has a very simliar crystallographic structure to α-N_2 (Cahill and Leroi, 1969), and, like α-N_2, the far-IR spectrum of α-CO consists of two narrow absorption lines (at 116 and 198 μm (Ron and Schnepp, 1967; Anderson and Leroi, 1966)).

Figure 4 shows the measured absorption coefficients for liquid CH_4 (Jones, 1970) and α-CO (Ron and Schnepp, 1967), as well as our fits to the data. Again, we employ an analytic approximation to the data because the measurements do not cover a broad enough wavelength range for us to calculate the integral in equation (5). The forms we use for the absorption coefficient spectra of CH_4 and α-CO as a function of wave number are respectively

$$\alpha_{CH_4} = 3.0e^{-[(\kappa-180)/78]^2}/2 \qquad (6a)$$

and

$$\alpha_{CO} = 4.7e^{-[(\kappa-50.5)/2.5]^2}/2 + 2.35e^{-[(\kappa-85.0)/5.5]^2}/2. \qquad (6b)$$

The peak absorption in CH_4 occurs at a wavelength of 55 μm, and the band is very broad (half-width of 78 cm^{-1}). The two α-CO lines at 116 and 198 μm (Ron and Schnepp, 1967; Anderson and Leroi, 1966) qualitatively resemble the α-N_2 lines, although in CO they are both stronger and somewhat wider. The α-CO spectrum was measured at temperatures of 7, 20 and 45 K with no temperature dependence reported for the strengths of the lines. The fit to the liquid CH_4 data is fairly good out to about 200 μm, beyond which our model obviously begins to overestimate the data. Also, the slope at wavelengths shorter than 40 μm is uncertain, although the rapid decline in the Planck function in this wavelength range makes our values of ε_b rather insensitive to the value of the absorption coefficients there. The fit to the α-CO data adequately describes the lines near their centers, but probably overestimates the absorption coefficients outside the lines.

Emissivity of mixtures

We modeled the effect of CO, CH_4, and photochemical products (which we considered as an arbitrarily introduced grey absorber) on the emissivity under a variety of model conditions. These models can be separated into two categories: those where the impurity exists as separate grains mixed intimately with the N_2 ice and those where the impurity is dispersed at the molecular level within the N_2 ice, i.e. solid solutions. In the case of CH_4 ice we also considered a third case, which was pure CH_4 ice on its own. We did not consider patchwork models of intermixed CH_4 and N_2 because the energy balance of CH_4 patches is probably independent of that for the N_2 patches (Stansberry *et al.*, 1996a). A situation where this might not be the case is for a veneer of CH_4 ice over the N_2 ice. We assess the importance of this possibility below.

The computation of the emissivity of a solid solution of N_2 and either CH_4 or CO is fairly straightforward if we assume that the absorption by molecules of each component is unaltered by being in close proximity to molecules of the other species. This assumption is reasonable for the spectrum of the N_2 because the presence of other molecules in dilute solution will not greatly perturb the N_2 lattice or the dynamics of most of the N_2 molecules in the lattice. However, it is probable that the spectrum of CH_4 and CO are changed by being dissolved in the N_2. We did not uncover any measurements of the far-IR absorption coefficients of N_2:CH_4 or N_2:CO solid solutions, and it is not clear how the guest molecules will contribute to the spectrum of the solid solution. Our approach is to simply add the absorption coefficients of CH_4 and/or CO, weighted by their mole fractions in the ice, to the absorption coefficients of the N_2. It may be that the true effect of the guest molecules will only be to slightly perturb the N_2 spectrum because these absorptions arise from the dynamics of the crystal lattice as much as from the dynamics of the individual molecules. We attempt to address this possibility to some degree by running some models using the absorption spectrum for β-CO (stable only above 61.6 K and modeled after the liquid CO coefficients from Jones (1970)), rather than the α-CO coefficients, to represent the absorption of CO in solid solution with β-N_2. In all of these models for solid solutions the addition of impurities increases the emissivity, although in many cases the increase is negligible.

We have also calculated the emissivity of intimate mixtures of the N_2 with grains of CH_4 and CO. Another intimate mixture we explored was of dark, fine particulates, perhaps photochemical products, dispersed amongst the N_2 grains. The computation of the emissivity of intimate mixtures follows Hapke (1993, equations (10.56)–(10.59)). These expressions give the effective single scattering albedo of a medium given the scattering efficiencies for the component particles, their abundances, and their sizes. The effective single scattering albedos are then used in equation (2) to calculate the emissivity of a mixture of the types of grains. As will be seen shortly, the bolometric emissivity of the N_2 can be either increased or decreased by the addition of contaminant grains composed of pure CH_4, CO or photochemical products, depending on the contaminant grain size.

Impact of impurities on ε_{N_2}

We explored a wide range of models which included impurities in the N_2 ice. The model parameters focus on relatively small concentrations of the contaminants because of the low abundances of CO and CH_4 determined from near-IR spectroscopy (Cruikshank *et al.*, 1993; Owen *et al.*, 1993). The abundance of material that is dark in the visible/near-IR (photochemical products) is also required to be quite small because it would be so effective at lowering the visible albedo. Our calculations indicate that at most there can be only a few percent of dark material ($w = 0.5$) in the N_2 ice, or the albedo would drop below the observed value of about 0.8. Mixtures of the contaminants with both α-N_2 and β-N_2 are considered. The temperatures we used for calculating the spectra and Planck means are 38 K for β-N_2 and 34 K for α-N_2 in all examples below.

Solid solution of CH_4 *and* β-N_2. A β-N_2 : CH_4 solid solution with a 10% CH_4 mixing ratio had bolometric emissivities of 0.42 and 0.88 for grain sizes of 0.1 and 1 cm, respectively. The corresponding emissivities of pure β-N_2 ice are 0.40 and 0.85. Smaller concentrations of CH_4 in the N_2, which are more relevant for Triton and Pluto, lead to even smaller changes in ε_b.

Solid solution of α-CO *and* β-N_2. A β-N_2 : CO solid solution with a 10% CO mixing ratio had bolometric emissivities of 0.40 and 0.85, the same as ε_b for pure N_2 ice. However, it is possible that a better model for this solid solution is to use the absorption coefficients for β-CO rather than α-CO (see below).

Solid solution of β-CO *and* β-N_2. Even though the temperatures we consider are well below the β–α phase transition temperature for CO, isolation of CO molecules in the β-N_2 matrix might result in the CO having a contribution to the spectrum more like that of β-CO than α-CO. We computed the emissivity of solid solutions of β-N_2 and β-CO. For a 10% mixing ratio of β-CO, ε_b increased from 0.40 to 0.43 in the case of 0.1 cm grains, and from 0.85 to 0.87 for 1 cm grains. This probably represents a fairly stringent upper limit on the effect of CO on the emissivity of β-N_2 ice on Triton and Pluto because of the large mixing ratio of CO employed.

Solid solution of CH_4 *and* α-N_2. A 34 K α-N_2 : CH_4 solid solution with a 10% CH_4 mixing ratio has bolometric emissivities of 0.25 and 0.67 for grain sizes of 0.1 and 1 cm, respectively. α-N_2 ice with a 2% CH_4 mixing ratio has bolometric emissivities of 0.15 and 0.45 at these grain sizes. The corresponding emissivities of pure α-N_2 ice at 34 K are 0.11 and 0.30. Thus CH_4 in α-N_2 increases the emissivity much more than it does in β-N_2. The emissivity of α-N_2 with some CH_4 in solution is greater than our calculation for pure α-N_2 indicates, but it is still considerably lower than the emissivity of β-N_2 at the same grain size. CH_4 also has an α form, which has two relatively narrow absorption features, much like α-CO and N_2. α-CH_4 is only stable below 20 K, but CH_4 isolated in an α-N_2 matrix might behave more like α-CH_4 than like β-CH_4. If this is the case then our calculations greatly overestimate the influence of CH_4 on the spectrum of an α-N_2:CH_4 solid solution, and the actual emissivity will be less than what we calculate.

Solid solution of α-CO *and* α-N_2. CO in α-N_2 has a greater influence on the emissivity than it does when dissolved in β-N_2. An α-N_2 : α-CO solid solution with a 10% CO mixing ratio has bolometric emissivities of 0.18 and 0.48 for 0.1 and 1 cm grain sizes (the pure α-N_2 values are 0.11 and 0.30). For a 2% mixing ratio of CO (more appropriate to Triton and Pluto), ε_b is increased to 0.13 and 0.35 for the 0.1 and 1 cm grain sizes.

Hypothetical molecular grey absorber in N_2. We added a grey absorption coefficient to equation (4a) (α_β). This models the effect of a hypothetical molecule, perhaps photochemically derived, with a wavelength independent absorption coefficient in solid solution with the N_2. The range of grey absorption coefficients we experimented with was $10^{-5} < \alpha_{grey} < 10^{-1}\,cm^{-1}$. The spectral emissivity increased, especially for the larger particle sizes, for $\alpha_{grey} > 10^{-4}$, but the bolometric emissivity did not increase appreciably until α_{grey} exceeded $10^{-2}\,cm^{-1}$. If the absorption coefficient of this hypothetical absorber in its pure form is taken to be $0.1\,cm^{-1}$, then it would only increase the bolometric emissivity for mixing ratios greater than about 10%.

Intimate mix of CH_4 *grains and* β-N_2. CH_4 grains in β-N_2 ice can either increase or decrease the bolometric emissivity. The size of CH_4 grains derived from modeling of near-IR spectra of Triton and Pluto is approximately 0.3 mm (T. Roush, personal communication), although the interpretation of this number is unclear because most of the CH_4 on both bodies is thought to be in solid solution with the N_2, not present as intermixed grains. Compounding that uncertainty is the complexity of the results for intimate mixes of CH_4 and β-N_2 grains. The single scattering albedos of 10, 100 μm and 1 mm CH_4 grains are 0.92, 0.99, and 0.88, while for 0.1 and 1 cm N_2 grains $w = 0.95$ and 0.51. Since the values of w for CH_4 are all greater than the 1 cm β-N_2 w, mixing them into the N_2 ice will actually decrease the emissivity. On the other hand, 10 μm and 1 mm CH_4 grains will increase ε_b when mixed with 0.1 cm β-N_2 grains, while 100 μm CH_4 grains decrease it. The maximum change in ε_b is for 100 μm CH_4 grains mixed with 1 cm N_2 grains: ε_b drops from 0.85 to 0.4 for a volume mixing fraction of 5% CH_4.

Intimate mix of CH_4 *grains with* α-N_2. Again, subject to the caveat that CH_4 is probably mostly in solid solution with N_2 on Triton and Pluto, we calculated the emissivity of intimately mixed grains of the two species. In this case the results are somewhat simpler than for mixes with β-N_2: with a single exception CH_4 grains increase ε_b for both N_2 grain sizes. For 100 μm CH_4 grains mixed with 1 cm N_2 grains ε_b decreases somewhat. For 0.1 cm α-N_2 grains ε_b increases from 0.11 to about 0.20 for 5% by volume of CH_4 grains. For 1 cm α-N_2 grains ε_b increases from 0.32 to about 0.43 with the addition of 5% by volume of 10 μm or 1 mm CH_4 grains, while 100 μm CH_4 grains decrease it to about 0.23.

Patches and coatings of CH_4. We have calculated the emissivity of pure CH_4 patches and estimated the importance of layers of CH_4 grains overlying N_2 ice. Figure 5 shows the emissivity of a half-space of CH_4 grains as a function of wavelength for several grain sizes. The emissivity tends to be higher than for N_2 ice because of the larger absorption coefficient of CH_4. The bolometric

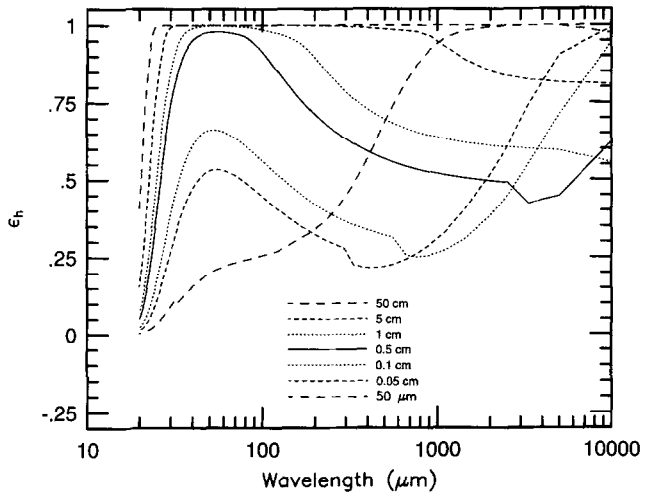

Fig. 5. The hemispherical emissivity of a surface composed of CH_4 grains as a function of wavelength for a number of grain sizes

emissivity of a pure CH_4 patch at 38 K is 0.55 for a grain size of 1 mm. This is larger than the value for pure β-N_2, $\varepsilon_b = 0.4$. As indicated earlier, the grain size of CH_4 on Triton and Pluto is rather unconstrained. Grundy (1995) derives grain sizes in the approximate range 0.1 mm to a few millimeters. Patches of CH_4 have been predicted on Triton and Pluto (Lunine and Stevenson, 1985; Stansberry *et al.*, 1996a) on the basis of volatile processes. If they are composed of grains smaller than about 1 cm they will have emissivities significantly less than one. N_2 ice with a layer of CH_4 on top of it is another likely configuration that may result from volatile processes (Spencer *et al.*, 1996; Stansberry *et al.*, 1996a; Trafton *et al.*, 1996). In this situation the CH_4 layer would increase the overall emissivity if its optical depth were significant. We estimate that this would be the case for layers of CH_4 thicker than about 2 cm, independent of the grain size of the CH_4.

Hypothetical dark (grey) particulates. We calculated the effect of dark particulates mixed with β-N_2 grains both on the albedo at 1 μm, which we take to be approximately 0.8, and on the bolometric emissivity. The dark particles were assigned single scattering albedos of 0.5 and sizes in the range $10 < a < 100\,\mu$m. The effect of dark fines such as these on the 1 μm albedo is extreme: for 10 μm fines mixed intimately with 1 cm N_2 grains the albedo drops below 0.8 for volume mixing ratios $> 1.3 \times 10^{-5}$. For 100 μm fines mixed with 0.1 cm N_2 grains, the volume mixing ratio can be no larger than 1.3×10^{-3}. We calculated the Planck mean single scattering albedos of the fines in the far-IR by assuming grey absorption coefficients for the material of 10 and $10^3\,cm^{-1}$. We then used the Planck mean single scattering albedos in the Hapke mixing formula to calculate the effective single scattering albedo for the medium, which was used in turn to calculate ε_b for the mixture. At the tiny volume mixing ratios of dark particles just discussed ($\lesssim 0.1\%$), there was essentially no effect on the bolometric emissivity of the N_2 ice. For larger mixing ratios the introduction of "dark" particulates can either increase or decrease the emissivity. If the particles were truly dark in the far-IR they would always increase the emissivity. However, the far-IR single scattering albedos of the fines we used were, in some cases, actually higher than the single scattering albedos of the N_2 grains. This was especially true for the 1 cm N_2 grains, which have a Planck mean single scattering albedo of only 0.51. The single scattering albedos of dark fines were frequently found to be higher than this value, resulting in lower values of ε_b for the mixture. Such was not the case for any of our test cases involving dark fines mixed with 0.1 cm N_2 grains, which have a mean single scattering albedo of 0.95. The emissivity of N_2 ice composed of these smaller grains was increased by the admixture of all dark particulates we considered, although at volume mixing ratios $\lesssim 0.1\%$ the effect on the emissivity for the 1 mm grain size was also negligible.

Discussion and conclusions

The range of bolometric emissivities we calculate for a pure β-N_2 ice surface at 38 K with a characteristic grain size in the range 0.1–1 cm is $\varepsilon_b = 0.40$–0.85. These results are in excellent agreement with the range of bolometric emissivities, 0.30–0.77, derived from Triton's albedo (as measured by the Voyager ISS). The re-analysis of Voyager IRIS data from Triton (Stansberry *et al.*, 1996b) in the 20–50 μm spectral range results in an emissivity of 0.42 ± 0.07. Our calculated spectral emissivity in that wavelength range is also quite low, ranging from nearly zero at 20 μm to between 0.2 and 0.5 for 0.1–1 cm grain sizes. The bolometric emissivity for pure α-N_2 is considerably lower than for β-N_2 at the same grain size. At 34 K we calculate that $0.11 < \varepsilon_b < 0.30$ for grain sizes 0.1–1 cm. While the emissivity of α-N_2 does not have any bearing on the current energy balance on Triton and Pluto, it could well come into play over the course of a season. We will return to this topic below.

We find that CH_4 or CO in solid solution with β-N_2 ice probably has little effect on the emissivity, at least at the low concentrations they are thought to be present on Triton and Pluto. Our calculations indicate that if both of these molecules are present at a mixing ratio of 10% the emissivities for 1 mm and 1 cm grain sizes increase by less than 10%. If we use the absorption spectrum of β-CO, which absorbs much more strongly than α-CO, the emissivities still increase no more than 10%. This probably represents an upper limit on the emissivity increase created by CH_4 and CO in solid solution with β-N_2 because both species are thought to be present at mixing ratios considerably lower than 10%.

On the other hand, CH_4 and/or CO in solid solution with α-N_2 can have an important effect on ε_b. If both are present at a mixing ratio of just 2%, the emissivity of α-N_2 increases by about 50%. For a 1 mm grain size ε_b jumps from 0.11 to 0.16, and for a 1 cm grain size it goes from 0.30 to 0.48. Accurately determining the mixing ratio of CH_4 and CO in Triton's and Pluto's N_2 ice will be very important for further constraining just what emissivity to expect for α-N_2 with those components in solid solution. However, it seems quite certain that the emissivity of α-

N_2, whether pure or with CH_4 and CO in it, is considerably lower than the emissivity of β-N_2 at the same grain size.

Our effort to characterize the effect of mixing CH_4 and CO grains with N_2 grains produced mixed results. Since the near-IR spectra indicate that these molecules are predominantly in solid solution with the N_2, we will not attempt to summarize our intimate mixing results here. However, the emissivity of CH_4 ice is of interest in its own right because volatile processes will tend to segregate it from the N_2 in some areas. It has been argued (Trafton and Stern, 1983) that CH_4 ice itself has a low emissivity. For CH_4 grain sizes of 0.1, 1, and 10 mm we calculate $\varepsilon_b = 0.25$, 0.55, and 0.95, respectively. Obviously it is important to consider the possibility that CH_4 ice has a low emissivity, and conversely it is important to try and constrain the grain size of any relatively pure CH_4 ice on Triton and Pluto. Intimate mixes of fine, dark particles with N_2 ice will have little effect on the emissivity because they cannot be present at volume mixing ratios greater than about 0.1%, or the N_2 ice would be darkened too much.

In addition to an uncertainty in the appropriate grain size to use in these calculations, there are other systematic uncertainties in our calculations. We have investigated the effects of nonisotropic single particle phase functions ($P(g) = 1 \pm \cos(g)$, where g is the phase angle) and find that the mean emissivities can vary by about 5% with phase function, with forward scattering particles having higher emissivities. However, the same argument that leads us to reduce Q_{ext} for large, closely spaced particles implies that the single particle phase function should be less important for the grain sizes we are primarily concerned with here. We also doubled the β-N_2 absorption coefficient and recalculated the emissivity. This also leads to approximately a 5% increase in ε_b. Based on these calculations we estimate that the systematic uncertainty in our emissivities for a given grain size are probably about $\pm 5\%$.

It is possible that Triton's, and presumably Pluto's, N_2 ice is overlain by a translucent, annealed layer (Eluszkiewicz, 1991). Such a layer is potentially important for the emissivity of the surface, especially if it contains few scatterers. If that is the case the effective grain size could be quite large, and if the annealed layer is deep (~ 10 cm), our calculations show that the emissivity would be close to unity. Eluszkiewicz, as well as Nelson *et al.* (1990a,b), also argued that ε_b should be large because roughness at scales larger than the wavelength of Triton's thermal radiation ($\sim 100\ \mu$m) would act as "cavity radiators", giving the surface an emissivity near unity. In fact roughness does not play a major role in determining the emissivity of a surface: rather, it is determined by the relative efficiencies of scattering and absorption within the surface (or within an atmosphere for that matter).

This is relatively simple to demonstrate. The unusual geometry of a cavity radiator (a chamber with opaque walls, and a hole which is small relative to the size of the chamber but large compared with the wavelength of the radiation being considered) creates a situation where the optical depth seen in any direction from within the cavity is infinite except at the small opening. The radiance at the opening is essentially an unaltered sample of the perfectly isotropic, thermalized radiation of the cavity's interior. A surface covered with cavity radiators cannot, in fact, have an emissivity of one because of the geometric requirements of the cavities, i.e. that the cavity be large compared to the opening. If the ratio of the size of the opening to the size of the cavity is 1/10, the maximum emissivity the surface can have is $\varepsilon_{max} \simeq (1/10)^2 = 0.01$. Thus, while the emissivity of the opening in a cavity radiator is defined as unity, the emissivity of a surface covered with cavity radiators would be much smaller, and ideally would approach zero, not one.

So far our discussion has focused on the bolometric emissivity, but the spectral emissivities we calculate are also of interest. Figure 2a reveals that the emissivity of β-N_2 is critical for understanding the full set of far-IR measurements of Pluto's brightness. The letters across the bottom of the figure indicate the wavelengths at which those measurements have been made. Troubles encountered in trying to fit all of the Pluto data with a single blackbody function lead Tryka *et al.* (1994) to use a model with 40 K, $\varepsilon_b = 0.6$ polar caps and an equatorial zone with temperature determined using a standard thermal model. Their model fluxes fall within the error bars of all of the far-IR observations, although the model falls just within the top of the error bars for all of the observations at $\lambda \geq 800\ \mu$m. Our calculations show that a single emissivity probably does not adequately describe the thermal emission from the polar caps, and that the long-wavelength emissivities should be considerably lower than near 100 μm. This would tend to correct the flux levels at long wavelengths in the Tryka *et al.* model, although we have not quantitatively assessed the effect. The emissivity at wavelengths shortward of 50 μm is also quite low. This has important implications for the measurements of Triton's emission made by Voyager 2. In particular, the recent conclusion of Stansberry *et al.* (1996b) that Triton's emissivity in the 20–50 μm wavelength range is approximately 0.4 is entirely consistent with these calculations. Further modeling of the infrared spectra of either Triton or Pluto would be improved by taking our spectral emissivities into account.

Our results for the emissivity of β-N_2 are important for the current thermal state of the surfaces of Triton and Pluto. Because their atmospheres are in vapor pressure equilibrium with the N_2 on the surface, the emissivity is also important for understanding their atmospheres. This is particularly true of Pluto. As mentioned in the introduction, the deepest level to which Pluto's atmosphere was probed in the 1988 occultation is 3 μb, which corresponds to the vapor pressure of N_2 at 35.2 K. Stansberry *et al.* (1994) found that this was also very close to the unit emissivity equilibrium temperature for N_2 on Pluto. So, one possibility is that the occultation just barely reached the surface, the surface pressure is 3 μb, and Pluto's radius is near 1200 km. However, the mutual-event radii for Pluto are considerably smaller, being about 1165 km. N_2 ice on the surface at that radius would have to be warmer than 35.2 K to be in vapor pressure equilibrium with the correspondingly deeper atmosphere. If we take the albedo of the N_2 ice to be the same in either scenario, then a low emissivity such as we calculate is a straightforward way to raise the temperature of the surface. The value of ε_b

required is about 0.6, which falls well within the range of values we calculate.

The results for α-N_2 are potentially of more interest than those for β-N_2, even though the surfaces of both Triton and Pluto appear to be comfortably within the β-N_2 temperature range at this time. In light of the strong seasonal forcing on both bodies that situation could easily change. Pluto provides a clearer example for showing this, because there the seasonal forcing is dominated by the large (0.25) orbital eccentricity. If we estimate Pluto's *c.* 1990 equilibrium temperature taking the bolometric albedo to be 0.8 and the emissivity to be 0.6, we obtain $T_e = 38.5$ K, assuming a 4π radiator. Extrapolating to Pluto's aphelion at nearly 50 AU, we obtain $T_e = 30$ K. The vapor pressure of N_2 at 30 K is 0.04 μb, three orders of magnitude lower than its current value: this is the atmospheric collapse first pointed out by Stern and Trafton (1984). However, 30 K is below the phase transition temperature for N_2, so the correct value of the emissivity to use at aphelion is that for α-N_2, not β-N_2. Taking $\varepsilon_b = 0.2$, based on our results for α-N_2, gives an equilibrium temperature at aphelion of $T_e = 39.3$ K, slightly greater than the perihelion temperature. The obvious resolution to this inconsistency is that at aphelion Pluto's surface is covered partly in β-N_2 and partly in α-N_2, with the β-N_2 occupying sunlit areas and α-N_2 occupying darker areas. Phase equilibrium and latent heat transport will then maintain the temperature of all of the N_2 ice at the phase transition temperature, $T_c = 35.6$ K. The vapor pressure of N_2 at this temperature is 4.2 μb, only slightly lower than the current surface pressure, even though the aphelion insolation is only 36% of the perihelion insolation. This mechanism may be able to prevent the freeze-out of Pluto's atmosphere, or at least significantly postpone it.

Acknowledgements. Will Grundy provided code for accurately calculating the *H* function, as well as many useful comments. Janusz Eluszkiewicz and Anne Verbiscer pointed out some inherent limitations to the calculations. Bruce Hapke, Larry Trafton and Robert (California) Brown provided excellent input as referees, as did Leslie Young and Ted Roush. J.S. thanks Lowell Observatory, where part of this work was performed under NASA grant NAGW-3395. J.S. and R.Y. acknowledge support through the National Research Council Associateship Program. D.P. was supported by the Research Experience for Undergraduates program, administered through the Northern Arizona University Physics and Astronomy Department.

References

Altenhoff, W. J., Chini, R., Hein, H., Kreysa, E., Mezger, P. G., Salter, C. and Schraml, J. B., First radio astronomical estimate of the temperature of Pluto. *Astron. Astrophys.* **190,** L15–L17, 1988.

Anderson, A. and Leroi, G. E., *J. Chem. Phys.* **45,** 4359, 1966.

Aumann, H. H. and Walker, R. G., IRAS observations of the Pluto–Charon system. *Astron. J.* **94,** 1088–1091, 1987.

Baran, B. W. and Medina, F. D., Far-infrared spectrum of solid methane. Phase II. *Chem. Phys. Lett.* **129,** 125–128, 1986.

Broadfoot, A. L., Atreya, S. K., Bertaux, J. L., Blamont, J. E., Dessler, A. J., Donahue, T. M., Forrester, W. T., Hall, D. T., Herbert, F., Holberg, J. B. *et al.*, Ultraviolet spectrometer observations of Neptune and Triton. *Science* **246,** 1459–1466, 1989.

Brown Jr, G. N. and Ziegler, W. T., Vapor pressure and heats of vaporization and sublimation of liquids and solids of interest in cryogenics below 1-atm pressure. *Adv. Cryogenic Engng* **25,** 662–670, 1980.

Brown, R. H. and Kirk, R. L., Coupling of internal heat to volatile transport on Triton. *J. Geophys. Res.* **99,** 1965–1981, 1994.

Buie, M. W., Tholen, D. J. and Horne, K., Albedo maps of Pluto and Charon: initial mutual event results. *Icarus* **97,** 211–227, 1992.

Buontempo, U., Cunsolo, S., Dore, P. and Maselli, P., Far infrared absorption spectra of β-solid nitrogen. *Phys. Lett.* **74A,** 113–115, 1979.

Cahill, J. E. and Leroi, G. E., Raman spectra of solid CO_2, N_2O, N_2, and CO. *J. Chem. Phys.* **51,** 1324–1332, 1969.

Conrath, B., Flasar, F. M., Hanel, R., Kunde, V., Maguire, W., Pearl, J., Pirraglia, J., Samuelson, R., Gierasch, P., Weir, A., Bezard, B., Gautier, D., Cruikshank, D. *et al.*, Infrared observations of the Neptunian system. *Science* **246,** 1454–1459, 1989.

Cruikshank, D. P., Roush, T. L., Owen, T. C., Geballe, T. R., de Bergh, C., Schmitt, B., Brown, R. H. and Bartholomew, M. J., Ices on the surface of Triton. *Science* **261,** 742–745, 1993.

Drish Jr, W. F., Harmon, R. H., Marcialis, R. L. and Wild, W. J., Images of Pluto generated by matrix lightcurve inversion. *Icarus* **113,** 360–386, 1995.

Elliot, J. L. and Young, L. A., Analysis of stellar occultation data for planetary atmospheres. I. Model fitting with application to Pluto. *Astron. J.* **103,** 991, 1992.

Elliot, J. L., Dunham, E. W., Bosh, A. S., Slivan, S. M., Young, L. A., Wasserman, L. H. and Millis, R. L., Pluto's atmosphere. *Icarus* **77,** 148–170, 1989.

Eluszkiewicz, J., On the microphysical state of the surface of Triton. *J. Geophys. Res. (Suppl.)* **96,** 19217–19229, 1991.

Grundy, W. M., Methane and nitrogen ices on Pluto and Triton: a combined laboratory and telescope investigation. Ph.D. Dissertation, University of Arizona, 1995.

Grundy, W. M. and Fink, U., The absorption coefficient of the liquid N_2 2.15 μm band and application to Triton. *Icarus* **93,** 169–173, 1991.

Grundy, W. M., Schmitt, B. and Quirico, E., The temperature-dependent spectra of α and β nitrogen ice with application to Triton. *Icarus* **105,** 254–258, 1993.

Gurrola, E. M., Interpretation of radar data from the icy Galilean satellites and Triton. Ph.D. Dissertation, Stanford University, 1995.

Hapke, B. W., Bidirectional reflectance spectroscopy, 1: Theory. *J. Geophys. Res.* **86,** 3039–3054, 1981.

Hapke, B. W., Bidirectional reflectance spectroscopy, 4: Extinction and the opposition effect. *Icarus* **67,** 41–59, 1986.

Hapke, B. W., *Theory of Reflectance and Emittance Spectroscopy*. Cambridge University Press, Cambridge, 1993.

Hillier, J., Helfenstein, P., Verbiscer, A., Veverka, J., Brown, R. H., Goguen, J. and Johnson, T. V., Voyager disk-integrated photometry of Triton. *Science* **250,** 419–421, 1990.

Hillier, J., Helfenstein, P., Verbiscer, A. and Veverka, J., Voyager photometry of Triton: haze and surface photometric properties. *J. Geophys. Res.* **96,** 19203–19210, 1991.

Hiroi, T., Recalculation of the isotropic *H* functions. *Icarus* **109,** 313–317, 1994.

Hubbard, W. B., Hunten, D. M., Dieters, S. W., Hill, K. M. and Watson, R. D., Occultation evidence for an atmosphere on Pluto. *Nature* **336,** 452–454, 1989.

Hubbard, W. B., Yelle, R. V. and Lunine, J. I., Nonisothermal Pluto atmosphere models. *Icarus* **84,** 1–11, 1990.

Ingersoll, A. P., Dynamics of Triton's atmosphere. *Nature* **344,** 315–317, 1990.

Jewitt, D. C., Heat from Pluto. *Astron. J.* **107,** 372–378, 1994.

Jones, M. C., Far infrared absorption in liquefied gasses. Natl Bur. Stand. Tech. Note 390, 1970.

Lunine, J. I. and Stevenson, D. J., Physical state of volatiles on the surface of Triton. *Nature* **317,** 238–240, 1985.

McEwen, A. S., Global color and albedo variations on Triton. *Geophys. Res. Lett.* **175,** 1765–1768, 1990.

Millis, R. L., Wasserman, L. H., Franz, O. G., Nye, R. A., Elliot, J. L., Dunham, E. W., Bosh, A. S., Young, L. A., Slivan, S. M., Gilmore, A. C., Kilmartin, P. M., Allen, W. H., Watson, R. D., Dieters, S. W., Hill, K. M., Giles, A. B., Blow, G., Priestley, J., Kissling, W. M., Walker, W. S. G., Marino, B. F., Dix, D. G., Page, A., Ross, J. E., Kennedy, H. D. and Klemola, A. R., Pluto's radius and atmosphere: results from the entire 9 June 1988 occultation data set. *Icarus* **105,** 282–297, 1993.

Nelson, R. M., Buratti, B. J., Wallis, B. D., Smythe, W. D., Horn, L. J., Lane, A. L., Mayo, M. J. and Simmons, K. E., Spectral geometric albedo and bolometric bond albedo of Neptune's satellite Triton from Voyager observations. *Geophys. Res. Lett.* **17,** 1761–1764, 1990a.

Nelson, R. M., Smythe, W. D., Wallis, B. D., Horn, L. J., Lane, A. L. and Mayo, M. J., Temperature and thermal emissivity of the surface of Neptune's satellite Triton. *Science* **250,** 429–431, 1990b.

Owen, T. C., Roush, T. L., Cruikshank, D. P., Elliot, J. L., Young, L. A., deBergh, C., Schmitt, B., Geballe, T. R., Brown, R. H. and Bartholomew, M. J., Surface ices and atmospheric composition of Pluto. *Science* **261,** 745, 1993.

Prokhvatilav, A. I. and Yantsavich, L. D., *Sov. J. Low Temp. Phys.* **9,** 94–97, 1983.

Reinsch, K., Burwitz, V. and Festou, M. C., Albedo maps of Pluto, and improved physical parameters of the Pluto–Charon system. *Icarus* **108,** 209–218, 1994.

Ron, A. and Schnepp, O., Lattice vibrations of the solids N_2, CO_2, and CO. *J. Chem. Phys.* **46,** 3991–3998, 1967.

St. Louis, R. V. and Schnepp, O., Absolute far-infrared absorption intensities of α-nitrogen. *J. Chem. Phys.* **50,** 5177–5183, 1969.

Savoie, R. and Fournier, R. P., Far-infrared spectra of condensed methane and methane-d_4. *Chem. Phys. Lett.* **7,** 1–3, 1970.

Scott, T. A., Solid and liquid nitrogen. *Physics Reports* **27,** 89–157, 1976.

Smith, B. A., Sodderblom, L. A., Banfield, D., Barnet, C., Basilevsky, A. T., Beebe, R. F., Bollinger, K., Boyce, J. M., Brahic, A., Briggs, G. A., Brown, R. H. *et al.*, Voyager 2 at Neptune: imaging science results. *Science* **246,** 1422–1449, 1989.

Spencer, J. R., Trafton, L. M., Stansberry, J. A., Young, E. F., Binzel, R. P. and Croft, S. K., Volatile transport, seasonal cycles, and atmospheric dynamics on Pluto, in *Pluto and Charon* (edited by S. A. Stern and D. J. Tholen). University of Arizona Press, Tucson, 1996 (in press).

Stansberry, J. A., Surface–atmosphere coupling on Triton and Pluto. Ph.D. Dissertation, University of Arizona, Tucson, 1994.

Stansberry, J. A., Lunine, J. I., Porco, C. C. and McEwen, A. S., Zonally averaged thermal balance and stability models for Triton's polar caps. *Geophys. Res. Lett.* **17,** 1773–1776, 1990.

Stansberry, J. A., Yelle, R. V., Lunine, J. I. and McEwen, A. S., Triton's surface–atmosphere energy balance. *Icarus* **99,** 242–260, 1992.

Stansberry, J. A., Lunine, J. I., Hubbard, W. B., Yelle, R. V. and Hunten, D. M., Mirages and the nature of Pluto's atmosphere. *Icarus* **111,** 503–513, 1994.

Stansberry, J. A., Spencer, J. R., Schmitt, B., Benchkoura, A., Yelle, R. V. and Lunine, J. I., A model for the overabundance of methane in the atmospheres of Pluto and Triton. *Planet. Space Sci.* **44,** 1051–1063, 1996a.

Stansberry, J. A., Spencer, J. R. and Pearl, J. C., Triton's temperature and emissivity: Voyager 2 IRIS data revisited. Submitted to *J. Geophys. Res.* 1996b.

Stern, S. A. and Trafton, L. M., Constraints on bulk composition, seasonal variation, and global dynamics of Pluto's atmosphere. *Icarus* **57,** 231–240, 1984.

Stern, S. A., Weintraub, D. A. and Festou, M. C., Evidence for a low surface temperature on Pluto from millimeter-wave thermal emission measurements. *Science* **261,** 1713–1716, 1993.

Sykes, M. V., Cutri, R. M., Lebofsky, L. A. and Binzel, R. P., IRAS serendipitous observations of Pluto and Charon. *Science* **237,** 1376–1380, 1987.

Tedesco, E. F., Veeder, G. J., Dunbax, R. S. and Lebofsky, L. A., IRAS constraints on the sizes of Pluto and Charon. *Nature* **327,** 127–129, 1987.

Thompson, W. R. and Sagan, C., Color and chemistry on Triton. *Science* **250,** 415–418, 1990.

Trafton, L. and Stern, S. A., On the global distribution of Pluto's atmosphere. *Astrophys. J.* **267,** 872–881, 1983.

Trafton, L., Matson, D. L. and Stansberry, J. A., Surface/atmosphere interaction and volatile transport (Triton, Pluto and Io), in *Solar System Ices* (edited by B. Schmitt, C. deBergh and M. Festou). Kluwer Academic, Dordrecht, Astrophys. Space Sci. Lib., 1996.

Tryka, K. A., Brown, R. H., Anicich, V., Cruikshank, D. P. and Owen, T. C., Spectroscopic determination of the phase composition and temperature of nitrogen ice on Triton. *Science* **261,** 751–754, 1993.

Tryka, K. A., Brown, R. H., Cruikshank, D. P., Owen, T. C., Geballe, T. R. and DeBergh, C., Temperature of nitrogen ice on Pluto and its implications for flux measurements. *Icarus* **112,** 513–527, 1994.

Tyler, G. L., Sweetnam, D. N., Anderson, J. D., Borutzki, S. E., Campbell, J. K., Eshleman, V. R., Gresh, D. L., Gurrola, E. M., Hinson, D. P. *et al.*, Voyager radio science observations of Neptune and Triton. *Science* **246,** 1466–1473, 1989.

Van de Hulst, H., *Light Scattering by Small Particles.* Wiley, New York, 1957.

Yelle, R. V., Lunine, J. I. and Hunten, D. M., Energy balance and plume dynamics in Triton's lower atmosphere. *Icarus* **89,** 347–358, 1991.

Yelle, R. V., Lunine, J. I., Pollack, J. and Brown, R. H., Volatile transport and lower atmospheric structure on Triton, in *Neptune and Triton* (edited by D. Cruikshank). University of Arizona Press, Tucson, 1995.

Young, E. F., An albedo map and frost model of Pluto. Ph.D. Dissertation, Massachusetts Institute of Technology, 1993.

Young, E. L. and Binzel, R. P., A new determination of radii and limb parameters for Pluto and Charon from mutual event lightcurves. *Icarus* **108,** 219–224, 1994.

Young, L. A., Bulk properties and atmospheric structure of Pluto and Charon. Ph.D. Dissertation, Massachusettes Institute of Technology, 1994.